Analytica Chimica Acta 1102 (2020) 99–108

Contents lists available at ScienceDirect

Analytica Chimica Acta

journal homepage: www.elsevier.com/locate/aca

A red-shifted Bioluminescence Resonance Energy Transfer (BRET) biosensing system for rapid measurement of plasmin activity in human plasma

Felix Weihs [a, *], Alex Peh [b, c, 1], Helen Dacres [a]

[a] CSIRO, Food Innovation Centre, 671 Sneydes Road, Werribee, VIC, 3030, Australia
[b] CSIRO, Black Mountain Laboratories, Clunies Ross Street, ACTON, Canberra, ACT, 2601, Australia
[c] Universiti Putra Malaysia, Malaysia

HIGHLIGHTS

- Signal and protease sensing sensitivity comparison between blue ($BRET^2$) and red-shifted ($BRET^6$) BRET in human plasma.
- Improved protease recognition site for sensing human plasmin activity with high specificity and sensitivity.
- $BRET^6$-based sensor is faster and more specific compared to a commercially available system.
- A rapid assay (10 min) can be used to cover biologically relevant activities of plasmin.

GRAPHICAL ABSTRACT

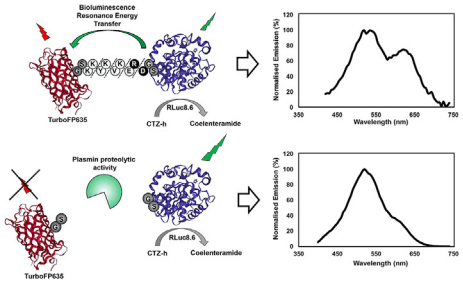

ARTICLE INFO

Article history:
Received 2 October 2019
Received in revised form
20 November 2019
Accepted 16 December 2019
Available online 18 December 2019

Keywords:
Bioluminescence resonance energy transfer
Protease activity
Plasmin
Human plasma
Bioluminescence
Fibrinolysis

ABSTRACT

Proteases are key signalling molecules for many physiological processes and their dysregulation is implicated in the progression of a range of diseases. Sensitive methods to measure protease activities in complex biological samples are critical for rapid disease diagnoses. The proteolytic activity of plasmin reflects the fibrinolysis state of blood and its deregulation can indicate pathologies such as bleeding events. While Bioluminescence Resonance Energy Transfer (BRET) is a powerful and sensitive method for the detection of protease activity, the commonly applied blue-shifted $BRET^2$ system, consisting of the *Renilla* luciferase Rluc2 and the large-stokes shift fluorescent protein GFP^2, suffers from light absorption and light scattering in human plasma samples. To address this challenge, we developed a red-shifted BRET-based plasmin sensor by substituting $BRET^2$ with the $BRET^6$ system. $BRET^6$ is composed of the red-shifted RLuc8.6 luciferase linked to the red light emitting fluorescent protein TurboFP635. The $BRET^6$ biosensor exhibited 3-fold less light absorption in plasma samples compared to the $BRET^2$ sensor leading to an up to a 5-fold increase in sensitivity for plasmin detection in plasma. The limits of detection for plasmin were determined to be 11.90 nM in 7.5% (v/v) plasma with a 10 min assay which enables biologically relevant plasmin activities of thrombolytic therapies to be detected. While a colorigenic plasmin activity assay achieved a similar detection limit of 10.91 nM in 7.5% (v/v) human plasma, it required a 2 h incubation period. The $BRET^6$ sensor described here is faster and more specific than the colorigenic assay as it did not respond to unspiked human plasma samples.

* Corresponding author.
E-mail address: felix.weihs@csiro.au (F. Weihs).
[1] Present address: The University of Tokyo.

https://doi.org/10.1016/j.aca.2019.12.044
0003-2670/

1. Introduction

Proteases are of major importance in biomedical research and diagnostics with a great demand for rapid diagnostic tools. As most proteases are regulated on a post-translational level, abundance and activity can be significantly different which requires activity-based detection sensors. A good example of a tightly regulated system based on proteolytic activities is fibrinolysis [1]. Fibrinolysis is a complex system present in blood that controls the formation and dissolution of blood clots. Disturbing the haemostatic balance of the fibrinolytic system can lead to complications ranging from thrombosis to more severe pathologies such as major bleeding or intracranial haemorrhages that are major causes for mortality. While thrombolytic agents, such as the plasminogen activators Alteplase and Reteplase, aim to dissolve dangerous blood clots during thrombosis, no available agents allow site-specific activation of fibrinolysis at the clot but instead lead to systemic plasminogen-activation that can result in bleeding events [1]. In order to improve thrombolytic treatments a number of diagnostics tools have been developed to monitor the fibrinolytic state. Assays that have been developed to detect fibrinolytic components such as plasminogen activators (tPA), inhibitors (PAI-1, α2-AP) [2], or fibrin degradation products remain poor indicators for bleeding risks potentially due to the complex nature of the fibrinolytic protein haemostasis [3,4]. The downstream effect of the fibrinolytic system leads to the modulation of plasmin activity making it the principal determinant for the fibrinolytic state and thus a highly interesting indicator for monitoring fibrinolytic state to facilitate adjustment of thrombolytic treatments.

Plasmin is a serine-protease responsible for the breakdown of polymerised fibrin and thus dissolves blood clots [5]. Plasmin activity can be measured using colorigenic or fluorogenic peptides that upon cleavage either results in an increase in absorbance at 405 nm [6] or fluorescence emission at 500 nm [7]. However, several dilutions to the sample are required as blood plasma typically shows high background fluorescence and excitation light scattering due to molecules present in blood such as haemoglobin.

Bioluminescence Resonance Energy Transfer (BRET)-based assays have proven to be an excellent choice to detect protease activity due to their high sensitivity and low background signal as no external illumination is required [8,9]. We previously developed BRET-based protease sensors specific for detecting thrombin and caspase-3. A BRET sensor was achieved a limit of detection (LOD) of 0.22 nM for sensing thrombin, 50 times more sensitive than the LOD of a comparable Förster Resonance Energy Transfer (FRET) sensor [10,11].

Recently, we developed a BRET biosensor to detect plasmin activity in milk as an indicator for milk spoilage [12]. This biosensor employs the BRET^2 combination using the *Renilla* luciferase variant RLuc2 catalysing a blue-shifted coelenterazine substrate (CTZ400a) donor system linked to the large-stokes-shift GFP variant GFP^2 acceptor via a peptide target sequence incorporating a plasmin recognition site. The sensor achieved a low limit of detection of 0.25 nM plasmin in 50% full fat UHT milk with a 10 min assay. Due to the sensor's good performance in milk, we set out to test its applicability in another complex liquid, human plasma.

However, unlike milk, human plasma contains metalloproteins such as haemoglobin that absorb light in a wavelength depending manner with increasing absorbance towards shorter wavelengths with a local maximum at ~410 nm [13] that overlaps well with the emission profile of RLuc2/CTZ400a. In addition, the short wavelength emission of BRET^2 is also subject to substantial light-scattering. Both effects together heavily affect the applicability of BRET^2 in human plasma. A red-shifted BRET system which can achieve the same protease sensing sensitivity of the BRET^2-plasmin sensor while circumventing light absorbance and scattering problems could be a powerful tool for detecting plasmin activity used to monitor the fibrinolysis state of patients.

In recent years, many red-shifted systems became available [14]. Li et al. demonstrated a functional BRET system composed of the *Gaussia* luciferase hGLuc linked to the red-light emitting fluorescent protein dimer tdTomato in diluted human serum [15]. While Ni and Arts successfully applied and detected NanoLuc luciferase-based (termed LUMABS) fusions with the fluorescent protein mNeonGreen [16] or the organic dye Cy3 [17] in human plasma samples using a smart phone. Another study used a red-shifted Firefly luciferase conjugated to the far-red light emitting organic dyes AlexaFluor™ 680 which could detect protease activity in whole blood [18].

As BRET^2 has been shown to be excellent protease sensing backbone which potentially exhibits a favourable conformation that allows proteases to access protease recognition sites situated between the luciferase and the acceptor fluorescent protein, we chose to replace the BRET^2 components in the BRET^2-PLR sensor with a BRET^6 combination. BRET^6 components are structurally similar and of a similar size to those of BRET^2 as RLuc2 is replaced by the red-shifted RLuc variant RLuc8.6 and GFP^2 is substituted with TurboFP635, a GFP-like fluorescent protein [19]. The BRET^6 components generate emission peaks (535 nm and 635 nm) that are more red-shifted than those of LUMABS (460 and 517/565 nm) and thus, are expected to be less affected by light attenuation in human plasma.

In the work presented here, the advantage of substituting BRET^2 with the red-shifted BRET combination BRET^6 [19] to detect plasmin activity levels directly in human plasma was investigated. The sensor performance was also compared with a commercially available plasmin activity test and we analysed factors influencing accurate plasmin detection in human plasma. This is the first report for a direct comparison of blue/red-shifted BRET system for the analysis of plasmin activities in human plasma with the first application of BRET^6 as a protease sensor. In addition, a new and optimised plasmin recognition site is used in this study.

2. Experimental

2.1. Chemicals

All chemicals used in this study were purchased from New England Biolabs (Genesearch, Australia), Biostrategy (Australia), Merck-Sigma-Aldrich (Australia), Macrogen (South Korea), GE Healthcare (Australia) or ThermoFisher Scientific (Australia). BRET analyses and treatment reactions were performed in phosphate buffered saline (10 mM Na_2HPO_4, 1.8 mM KH_2PO_4, 137 mM NaCl, 2.7 mM KCl, pH7.4), plasmin cleavage buffer (CB) (50 mM Tris-HCl (pH8), 50 mM NaCl, 25 mM Lysine) or TE-buffer (10 mM Tris (pH8), 1 mM EDTA) as noted at the respective experiments. Plasmin (Lot# SLBR3185V), thrombin (Lot# SLBV2136) from human plasma, uPA (urokinase from human kidney cells; Lot# SLBK3445V), MMP-2 (Lot# 1208473-2), MMP-3 (Lot# 2G217783), MMP-7 (Lot# SLBS9841) and MMP-9 (Lot# 2872521) were purchased from Merck-Sigma-Aldrich (Australia). Lyophilised Human plasma was purchased from Merck-Sigma-Aldrich (P9523) and reconstituted

with ddH_20 before use. Alpha-2 AP deficient plasma was purchased from Banksia Scientific Company (Australia) (Lot# LP39-0007).

2.2. Cloning, expression and purification of BRET sensors and controls

BRET-protein overexpression plasmids were constructed by cloning genes into pRSET (ThermoFisher Scientific) using standard techniques. The original pRSET-BRET2-PL construct was cloned previously [12]. Constructs were expressed in *E. coli* BL21(DE3) cells (New England Biolabs, USA). These cells were subsequently harvested and lysed using a high-pressure homogeniser (Avestin EmulsiFlex-C5, ATA Scientific Instruments, Canada). His-tagged BRET proteins were purified from lysates using HisTrap HP 1 ml columns integrated into an ÄKTAxpress Fast Performance Liquid Chromatography system (GE Healthcare, Australia), dialysed against 50 mM Tris (pH8), 50 mM NaCl at 4 °C, snap-frozen and stored at −80 °C. For a detailed description of cloning procedures, please see the Supporting Information.

2.3. Instrumentation

Spectral scans and bioluminescence intensities were recorded with a CLARIOStar plate-reader (BMG LabTech, Australia). Spectral scans with 5 nm step widths were measured from 380 to 600 nm for $BRET^2$ and from 400 to 740 nm for $BRET^6$ using a gain offsetting of 3600 for both systems. Bioluminescence intensities for $BRET^2$ were recorded with 410-80 nm (Gain: 3300) and 515-30 nm (Gain: 4095) bandwidth filters (1400-LU-$BRET^2$ filter set) and $BRET^6$ bioluminescence intensities were recorded with 500-40 nm (Gain: 2900) and 705-70 nm (Gain 4095) bandwidth that were set with linear variable filter monochromators. $BRET^6$ bandwidths were selected to reduce the emission of the RLuc8.6/CTZ-h at wavelengths >670 nm.

Reactions were carried out in 1.5 ml tubes incubated in a dry heating block before reactions mixtures were transferred to white 96-well plates (Opti-Plate 96, PerkinElmer, Australia) for bioluminescence measurements. Fluorescence scans were performed in black 96-well plates (Nunc, ThermoFisher Scientific, Australia) and D-Val-Leu-Lys-pNitroanilide assays were performed in transparent 96-well plates (Nunc, ThermoFisher Scientific, Australia).

2.4. BRET measurements

BRET measurements were carried out in a final assay volume of 100 µl using a sensor concentration of 10 nM and varying amounts of plasmin and human plasma. After a 10 min incubation at 30 °C. 100 µM of Coelenterazine 400a (for $BRET^2$ reactions) and Coelenterazine-h (for $BRET^6$ reactions) substrates were prepared in plasmin cleavage buffer containing 10% EtOH (v/v). 5 µl of 100 µM substrate was added to the well and the bioluminescence signal recorded immediately. The ratio of the mean value of 10 consecutive measurements recorded with an integration time of 0.5 s for each measurement was used for calculating BRET ratio's.

2.5. Nitroanilide-based plasmin activity test

D-Val-Leu-Lys-pNitroanilide assays were performed as described by Rauh et al. (2014) with minor modifications [20]. The substrate (Batch # SLBR4741V) was reconstituted in 100 mM Tris-HCL (pH8.0) buffer to a concentration of 5 mM. Assays were carried out in a 100 µl volume in transparent 96-well plates using 40 µl substrate (final conc. 2 mM), 50 µl CB or diluted human plasma and 10 µl of varying concentrations of plasmin. The assay mixtures were then incubated in the CLARIOstar at 37 °C for 2 h recording optical densities at 490 nm and 405 nm every 2 min.

2.6. Data analysis

Data analysis was carried out using GraphPad Prism (version 7 for Windows, Graphpad Software, San Diego, California, USA), MARS Data Analysis Software (BMG LabTech, Australia) and Microsoft Excel.

2.6.1. BRET measurements

$BRET^2$ ratios were calculated as integrated emission intensity measured at 500–530 nm divided by integrated emission intensities at 370–450 nm (equation (1)).

$$BRET^2 - Ratio = \frac{\int_{500nm}^{530nm} I}{\int_{370nm}^{450nm} I} \quad (1)$$

$BRET^6$ ratios were calculated as integrated emission intensity measured at 670–740 nm divided by integrated emission intensities at 480–520 nm (equation (2)).

$$BRET^6 - Ratio = \frac{\int_{670nm}^{740nm} I}{\int_{480nm}^{520nm} I} \quad (2)$$

Taking integrated emission intensities from 480 to 520 nm and 670–740 nm was used to reduce bleed-through of the RLuc8.6 emission profile into the acceptor bandwidth. This combination resulted in the highest difference (5.7-fold) of BRET ratios, comparing intact $BRET^6$ and RLuc8.6 alone, among the tested combinations (Fig. S1) (see supplementary information for a detailed description of tested bandwidth combinations).

BRET ratios were normalised using GraphPad Prism (Version 7) with maximal BRET ratio corresponding to 100% and lowest BRET ratio corresponding to 0% using the normalisation function. Curves were fitted with log (agonist) vs normalised response curves with variable slopes. Data are reported as means ± standard deviation (SD) with sample sizes of n = 3. The calculation of the half maximal effective concentration (EC_{50}) and two-tailed unpaired t-tests were performed using GraphPad Prism. Statistical significance was defined with asterisks indicating the following p-values: *: $p < 0.05$; n.s.: $p > 0.05$. The lower limits of detection (LOD) were calculated as the BRET ratio of the blank plus 3 × standard deviation of the blank [21].

For validation experiments, human plasma samples were spiked with known amounts of plasmin followed by the protease analysis procedure described before (2.4. BRET measurements). BRET ratios from measurements were interpolated from the fitted calibration curves to determine plasmin concentrations.

2.6.2. Absorbance measurements

Nitroanilide absorbance values were normalised by subtracting the OD_{490} from OD_{405} and plotted against incubation time and between 20 min and 120 min and linear regression analysis was performed using Office Excel (Microsoft). The rate of change of absorbance (AU/min) was then used to plot calibration curves of plasmin activity (mean ± SD; n = 3).

3. Results and discussion

3.1. Optimisation of plasmin recognition site

We previously demonstrated a BRET^2-based plasmin biosensor for detecting plasmin activity in milk as an indicator for spoilage [12]. In the previous BRET-based plasmin biosensor, a lysine-rich plasmin recognition sequence was flanked by BRET^2 components, GFP^2 and RLuc2 (Fig. 1a). This biosensor demonstrated high sensitivity for detecting plasmin activity as analysed by the reduction in resonance energy transfer efficiency concomitant with the dissociation of the BRET components.

We measured the sensitivity of the plasmin sensor in plasmin cleavage buffer (CB) using a 10 min assay. The half maximal effective concentration (EC_{50}) was calculated to be 8.74 nM and the limit of detection for plasmin was calculated to be 0.99 nM (Fig. 1) (Table 1). Both, LOD and EC_{50} were higher than previously observed where a POLARstar® Optima (BMG-Labtech) plate-reader was used [12] which is likely instrumentation-dependent as measurements were performed on a CLARIOstar® plate-reader in this study. These instruments possess different wavelength filter systems that can influence the assay sensitivity. The CLARIOstar® operates with linear variable filter monochromators while the POLARstar® Optima relies on the optical band-pass filters.

Following this, we measured the sensitivity of the plasmin sensor in various dilutions of human plasma in CB. LOD and EC_{50} in 1.5% (v/v) human plasma increased by 14.1-fold (13.91 nM) and 5-fold (43.38 nM), respectively, compared to measurements in CB, while an increase of the LOD and EC_{50} of 70.4-fold (69.65 nM) and 13.3-fold (116.10 nM), respectively, was determined for measurements in 7.5% (v/v) human plasma. This shows that plasmin sensing in human plasma is substantially decreased.

Biologically relevant plasmin levels such as seen for Reteplase treatment, range from 324 nM (0.1 U/ml) to 1946 nM (0.6 U/ml) [22] and thus, the biosensor would not be sensitive enough for measuring plasmin concentrations in this range. In the first step towards increasing the plasmin sensor sensitivity we engineered an improved plasmin recognition site.

Bovine plasmin is closely related to its human form with 78.1% identical amino acids (Fig. S2). Bovine plasmin preferentially cleaves residues following lysine residues and to a lesser degree, following arginine residues [23,24]. The existing plasmin sensor employs a plasmin recognition site consisting of a combination of Lys-X motifs found in the bovine plasmin native substrate of casein (GSKKYKVKEGS; termed 'PL' site) [12] flanked by glycine and a serine residue (Fig. 1a). A substrate phage-display study on human plasmin suggests that plasmin exhibits preferences for arginine at the two amino acid positions following the cleavage site (P1' – P2') [25]. Adding an arginine residue could thus act as a cleavage site itself and support the other cleavage sites composed of lysines. In an attempt to enhance the sensitivity of our sensor, we analysed the effect of adding an Arg-X motif to the plasmin recognition site.

In order to investigate the effect of the addition of an Arg-X to the plasmin recognition site to the sensor sensitivity for detecting plasmin we constructed a BRET^2-based sensor (BRET^2-PLR) linked by the peptide linker sequence GSKKYKVKERDGS (termed 'PLR' site) (Fig. 1a). Performing calibration curves in CB resulted in the LOD decreasing 5.5-fold from 0.99 nM with the BRET^2-PL sensor to 0.18 nM with the BRET^2-PLR sensor (Fig. 1b, Table 1).

However, despite the enhanced sensitivity afforded with the BRET^2-PLR sensor, the plasmin activity analyses in diluted human plasma showed drastically decreased sensitivities compared to the response in buffer (Table 1). LODs in diluted human plasma increased by 320-fold in 7.5% (v/v) plasma compared to in buffer. The BRET^2-PLR sensor system would still not be capable of measuring biologically relevant plasmin levels in plasma samples.

3.2. Red-shifted BRET system performance under plasma conditions

The employed BRET^2 system suffers from highly decreased signal intensities under plasma conditions leading to low signal counts and subsequently unreliable measurements and low sensitivities. Substituting BRET^2 with the red-shifted BRET^6 components [19] could improve the signal and measurement performance by cloning the 'PLR site between RLuc8.6 and TurboFP635.

BRET^6 produces bioluminescence at emission peaks of 535 and 635 nm and is more red-shifted than BRET^2 which exhibits emission peaks at 410 and 510 nm, respectively (Fig. S3a). A BRET ratio of ~0.8 was determined using the BRET^6-PLR sensor (taking the ratio of peak intensity values at 635nm/535 nm) which indicates a moderate energy transfer efficiency compared to a BRET ratio of ~2 (510nm/410 nm) determined with the BRET^2-PLR sensor (Fig. S3a). This reduction in energy transfer could be attributed to a less favourable overlap between the RLuc8.6/CTZ-h emission and TurboFP635 excitation spectra (Fig. S3b) compared to that of RLuc2/CTZ400a emission spectrum with the GFP^2 excitation spectrum and/or less favourable orientation of dipoles [26,27].

For all further experiments we analysed BRET ratios by measuring the integrated bioluminescence for donor and acceptor emission signal intensities (see method section). The BRET^6-PLR ratio was determined to be 0.24 ± 0.001 (n = 3) in PBS and 0.25 ± 0.001 (n = 3) in CB. We then compared the effect of adding

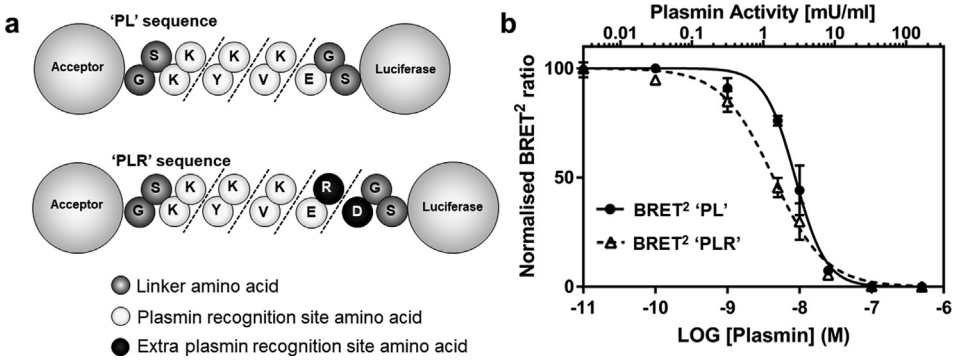

Fig. 1. Plasmin cleavage sensitivity dependent on recognition site in BRET^2.
a, schematic overview of both the PL and PLR recognition sites compared in this study. Dashed lines illustrate theoretical cleavage sites of plasmin. Grey blue circles illustrate flanking linker amino acids, white circles illustrate plasmin recognition site amino acids and black circle illustrate added amino acids for the 'PLR' recognition site. **b**, Log_{10} concentration response curves for 10 nM BRET^2-PL and BRET^2-PLR sensors with a human plasmin standard in plasmin cleavage buffer (mean ± SD, n = 3).

Table 1
BRET^2 and BRET^6-PLR Plasmin cleavage sensitivity
Limit of detection and EC_{50} were determined from Log_{10} concentration response curves from Fig. 5 and are shown as concentration and activity; nM (mU/ml). EC_{50} is the plasmin concentration for cleavage of half of the sensor. The linear range is defined as being between 10% and 90% of the maximal BRET response, respectively. All correlation coefficients are $R^2 < 0.98$. Abbreviations:α2-AP-def., α2-antiplasmin-deficient; inc., incubation; conc., concentration; LOD, Limit of detection; EC_{50}, half maximal effective concentration.

		Plasmin cleavage buffer	Plasmin cleavage buffer (30 min inc.)	Plasma (1.5% (v/v))	Plasma (7.5% (v/v))	α2−AP− def. Plasma (7.5% (v/v))
BRET^2-PL	LOD	0.99 (0.31)	N.D.	13.91 (4.3)	69.65 (21.53)	N.D.
	EC_{50}	8.74 (2.70)	N.D.	43.38 (13.41)	116.10 (35.89)	N.D.
	Linear Range	2.52−28.06	N.D.	63.13−267.28	79.92−168.72	N.D.
BRET^2-PLR	LOD	0.18 (0.06)	N.D.	10.12 (3.13)	57.60 (17.81)	N.D.
	EC_{50}	4.35 (1.34)	N.D.	42.40 (13.41)	129.90 (40.16)	N.D.
	Linear Range	0.73−27.72	N.D.	22.07−81.41	63.13−267.28	N.D.
BRET^6-PLR	LOD	0.14 (0.04)	0.08 (0.02)	1.11 (0.34)	11.90 (3.68)	1.12 (0.34)
	EC_{50}	1.12 (0.35)	0.48 (0.15)	3.69 (1.14)	69.74 (21.56)	7.11 (2.20)
	Linear Range	0.23−5.40	0.10−2.21	1.24−11.08	22.58−215.41	2.10−23.99

plasma to PBS on the bioluminescence signal intensity of the BRET^6 and BRET^2 sensors. BRET^6 donor signal intensity counts were 780401 ± 46522 (n = 3) in CB and 99275 ± 17491 (n = 3) in 7.5% (v/v) plasma retaining 12.7% of its intensity whereas the BRET^2 system donor counts reduced from 419923 ± 14468 (n = 3) in CB to 17016 ± 5369 (n = 3) in 7.5% (v/v) plasma resulting in only 4% residual signal intensity (Fig. 2a). The BRET^6 signal was thus significantly less (3x) attenuated than the BRET^2 signal in increasing amounts of plasma.

In addition, the BRET^6 ratio of 0.28 ± 0.001 (n = 3) recorded in 7.5% (v/v) plasma was similar to those recorded in PBS (0.24 ± 0.001; n = 3). The BRET^2 ratio significantly increased with increasing proportion of plasma (Fig. 2b). This effect could be due to the higher light attenuation of shorter-wavelength light compared to longer wavelength light (especially > 600 nm) in plasma which is mainly associated with haemoglobin absorption [13]. Taking these effects together gives BRET^6 an advantage over BRET^2 for applications in human plasma with regards to signal intensity.

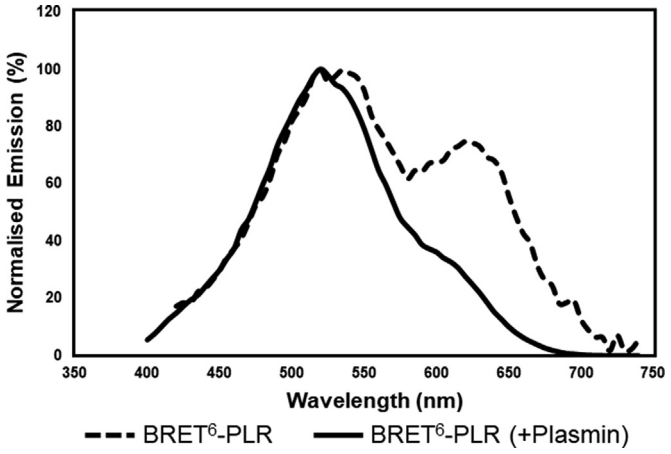

Fig. 3. Spectral analysis of BRET^6 Plasmin sensor in response to plasmin.
Emission spectra of 10 nM BRET^6-PLR incubated for 10 min at 30 °C with (solid line) or without 10 nM (dashed line) Plasmin. Spectra were normalised to peak emission.

3.3. *BRET^6 for plasmin sensing*

Incubation of the BRET^6 sensor with excess plasmin (10 nM) (in 100 µl, 3.09 mU/ml) at 30 °C for 10 min led to cleavage of the sensor as indicated by reduction in the emission peak at 635 nm (Fig. 3). No loss in donor signal was observed during incubation with plasmin (not shown) under the same conditions suggesting that plasmin does not cleave the RLuc8.6 luciferase.

This was further corroborated by SDS-PAGE analysis of cleaved products following incubation of the sensor with plasmin. SDS-PAGE analysis showed only two protein fragments corresponding to the sizes of RLuc8.6 (37.1 kDa) and TurboFP635 with the N-terminal purification tag (31.6 kDa) (Fig. 4a). The single bands at 40.3 kDa and 31.6 kDa for RLuc8.6 and TurboFP635, respectively, remained intact upon incubation with plasmin demonstrating they were not cleaved by plasmin (Fig. 4a). The size of purified RLuc8.6 is

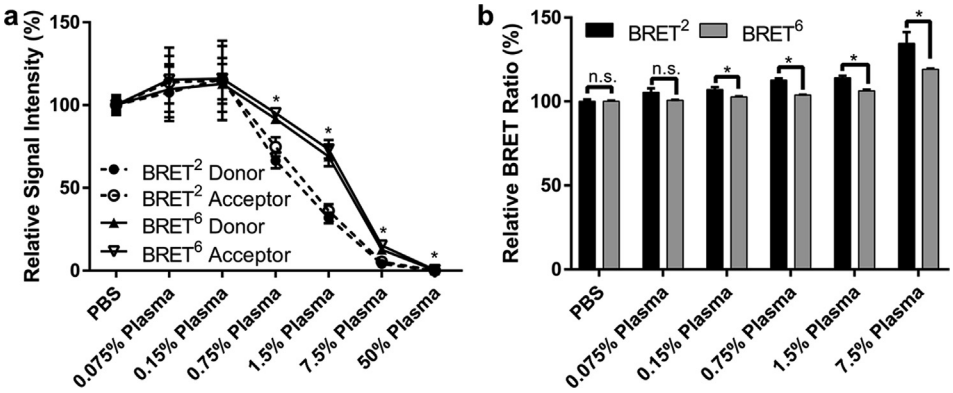

Fig. 2. Signal intensity and BRET ratio of the BRET^6 plasmin sensor and the BRET^2 plasmin sensor in human plasma.
a, Relative donor and acceptor signal intensities of BRET^2 and BRET^6 (mean ± SD; n = 3) relative to the sensor signal intensity in PBS. **b**, Relative BRET ratios (mean ± SD; n = 3) of BRET^2 and BRET^6 based plasmin sensors in different amounts of plasma (%, v/v) relative to BRET ratio in PBS. Statistical significance is indicated by an asterisk ($p < 0.05$) or no significance (n.s.) ($p > 0.05$).

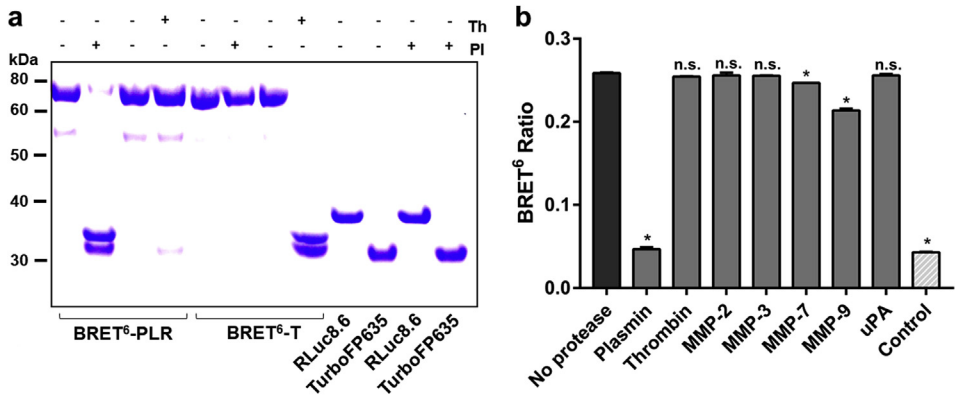

Fig. 4. BRET^6 Plasmin sensor specificity.
a, SDS-PAGE analysis of BRET^6-PLR, BRET^6-T and control constructs. 5 μg of sensors (BRET^6-PLR, BRET^6-T) and 2.5 μg of BRET^6-components (RLuc8.6, TurboFP635) were loaded per lane. All loaded proteins were pre-incubated for 10 min at 30 °C with 10 nM plasmin (Pl) (3.09 mU/ml) or 86 nM thrombin (Th) (100 U/ml) as indicated by the panel above the gel image. **b**, BRET ratio analysis (mean ± SD; n = 3) of plasmin sensor (BRET^6-PLR) and control proteins with and without the addition of protease. 10 nM of BRET^6-PLR or BRET^6-T sensor was incubated with 10 nM plasmin (3.09 mU/ml),17.2 nM thrombin (20 U/ml), 10 nM MMP-2, 10 nM MMP-3, 10 nM MMP-7, 10 nM MMP-9 or urokinase-type plasminogen activator (uPA) (20 U/ml) in plasmin cleavage buffer for 10 min at 30 °C. Controls consist of 10 nM of donor and acceptor molecules. Statistical significance was calculated against BRET^6-PLR without the addition of protease and is indicated by an asterisk ($p < 0.05$) or no significance (n.s.) ($p > 0.05$).

bigger than the corresponding cleavage product (40.3 kDa vs. 37.1 kDa) following incubation of the BRET^6 sensor with plasmin due to the presence of the N-terminal purification tag. This suggests that BRET^6 is a suitable sensor backbone for measuring plasmin activity.

There was an 80% reduction in the BRET^6 ratio from 0.25 ± 0.001 (n = 3) to 0.05 ± 0.004 (n = 3) upon incubation with 10 nM plasmin. An equimolar mix of purified RLuc8.6 and TurboFP635 resulted in a BRET^6 ratio of ~0.04 ± 0.001 (n = 3) which is similar to the BRET ratio of 0.05 ± 0.004 (n = 3) achieved following incubation with 10 nM plasmin for 10 min (Fig. 4b). This shows that BRET ratio of ~0.05 corresponds to full cleavage of the BRET^6 sensor.

3.4. Specificity and applicability in plasma

Analysing plasmin activity in human plasma exposes the sensor to a variety of other proteases such as thrombin, matrix metalloproteinases (MMPs) [28] or urokinase-type plasminogen activator (uPA) [29]. To investigate the specificity of the BRET^6-PLR sensor the sensor was incubated at 30 °C in 7.5% (v/v) plasma and the BRET^6 ratios were monitored over a 30-min period (Fig. S4). The BRET^6 ratio was shown to be independent of the incubation time and remained constant over the 30-min period. A BRET^6 ratio of ~0.3 corresponds to the response of the intact sensor in 7.5% (v/v) plasma. This illustrates that there are no proteases present in the tested plasma samples that can cleave the protease recognition site of the BRET^6-PLR or the individual BRET^6 components.

Both plasmin and thrombin, exhibit very high activities during fibrinolysis and thrombosis [30], respectively. It is thus important that the sensor construct can differentiate between the two proteases. This was tested by replacing the plasmin specific recognition site (GSKKYKVKERDGS) in BRET^6-PLR sensor with a thrombin recognition site (GSLVPRGS) enabling the direct comparison of the BRET^6 sensor to monitor plasmin (BRET^6-PLR) and thrombin (BRET^6-T) activity.

The BRET^6 sensors were incubated with, or without, the addition of 17.20 nM thrombin (2 U) for 10 min at 30 °C and analysed by SDS-PAGE (Fig. 4a). BRET^6-PLR remained mainly un-cleaved with and without the addition of thrombin with a prominent protein fragment being observed at ~68 kDa and a weaker band at 31.6 kDa corresponding to the predicted mass of TurboFP635. When BRET^6-T was incubated with thrombin, two fragments at ~37 kDa and 32 kDa corresponding to RLuc8.6 and His-tagged TurboFP635 were observed. A single protein band at ~68 kDa was observed when BRET^6-T was incubated with, and without, the addition of 10 nM plasmin demonstrating that BRET^6-T was not cleaved by plasmin.

Since a weak band at 31.6 KDa was be observed using SDS-PAGE analysis upon incubation of BRET^6-PLR with thrombin, we further investigated BRET^6-PLR cleavage by thrombin using BRET ratio analyses (Fig. 4b). The respective BRET ratios were 0.25 ± 0.002 (n = 3) and 0.26 ± 0.005 (n = 3) for BRET^6-PLR incubated (10 min, 30 °C) with, and without, the addition of thrombin. There was no significant difference ($P > 0.05$) between these BRET^6 ratios. In addition, the effect of other proteases that can occur in their active form in human plasma was studied by testing BRET ratios of BRET^6-PLR after incubation in presence of MMP-2 (10 nM), MMP-3 (10 nM), MMP-7 (10 nM), MMP-9 (10 nM) and uPA (20 U/ml) (Fig. 4b). The addition of MMP-2, MMP-3 and uPA demonstrated similar BRET ratios of 0.26 ± 0.003, 0.26 ± 0.001 and 0.26 ± 0.002 (all, n = 3), respectively, which were not significantly different to untreated BRET^6-PLR. Treatment with MMP-7 and MMP-9 resulted in significantly decreased BRET ratios of 0.25 and 0.21 ± 0.002 (both, n = 3), respectively. This shows that MMP-7 and MMP-9 exhibit a small proteolytic activity, albeit at high concentrations, on the sensor, while MMP-2, MMP-3 and uPA do not cleave the sensor. In conclusion, SDS-PAGE and BRET ratio analyses both confirm that the BRET^6-PLR sensor is specific for plasmin.

3.5. Cleavage over time

To enable comparison with previous studies and maintain a rapid protease sensing setup, a 10 min assay time was used for preliminary characterisation studies of BRET^6-PLR. We investigated the effect of extending the incubation time up to 30 min on the sensor sensitivity. In order to do so, a plasmin concentration of 1 nM was used as this concentration did not achieve full cleavage of the sensor within a 10 min incubation time.

SDS-PAGE analysis of BRET^6-PLR cleavage with 1 nM plasmin demonstrated a continuous cleavage of BRET^6 into its individual BRET^6 components. SDS-PAGE analysis only showed the appearance of protein bands corresponding to the predicted mass of RLuc8.6 (37.1 kDa) and TurboFP635 (31.6 kDa) illustrating that plasmin does cleave either BRET component even at prolonged incubation times (Fig. 5a). BRET ratio analysis demonstrated that

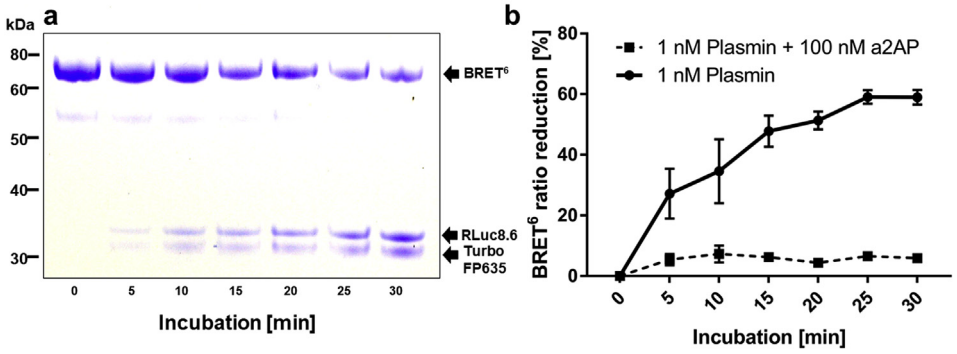

Fig. 5. Plasmin cleavage of BRET^6-PLR sensor as a function of time.
a, SDS-PAGE analysis of 5 μg BRET^6-PLR protein following incubation with 1 nM plasmin (0.31 mU/ml) for 0–30 min at 30 °C. Black arrows indicate band sizes of BRET^6-PLR, RLuc8.6 and TurboFP635. **b**, BRET ratio analysis of BRET^6-PLR (mean ± SD; n = 3) following incubation with 1 nM plasmin (0.31 mU/ml) for 0–30 min at 30 °C, with or without 100 nM α2-Antiplasmin (a2AP).

the BRET response plateaus following 25 min incubation with 1 nM plasmin (Fig. 5b). However, the sensor was not fully cleaved using 1 nM plasmin as the largest reduction in BRET ratio was ~60% while previous assays using 10 nM plasmin demonstrated a maximum BRET^6 ratio reduction of ~80% (Fig. 4b). This difference in response could be explained by substrate inhibition of plasmin sticking to the sensor after the proteolytic cleavage. Assay sensitivity could be improved up to ~50% if required by increasing the incubation time from 10 to 25 min. For BRET analysis, a control experiment was performed to corroborate whether the observed decrease in BRET ratio upon incubation of BRET^6-PLR with plasmin is due to the activity of plasmin or whether the incubation at 30 °C contributes to a loss of BRET ratio, potentially by sensor denaturation and/or impaired enzyme functions. This was performed by supplementing the 1 nM plasmin assay buffer with 100 nM of the plasmin-specific inhibitor protein α2-Antiplasmin (α2-AP) (Fig. 5b). α2-AP forms a reversible complex with plasmin by occupying the lysine-binding site of plasmin which in turn prevents plasmin from interacting with its substrates [31]. Importantly, no reduction in BRET^6-ratio was observed when 100 nM α2-AP was added to the plasmin cleavage buffer leading to the conclusion that BRET^6-PLR remains stable at 30 °C for at least 30 min in the tested buffer (CB) and the reduction in BRET ratio upon incubation with plasmin can be attributed to the proteolytic activity of plasmin.

3.6. Plasmin cleavage sensitivity

We next investigated whether the improvement in signal attenuation in human plasma observed when replacing the BRET^2 components with BRET^6 components in the BRET^2-PLR sensor (Fig. 2a) also translates into improved sensitivity for plasmin detection in plasma.

Calibration curves for plasmin were performed with BRET^2-PLR and BRET^6-PLR sensors in plasmin cleavage buffer, supplemented with 1.5% (v/v) plasma and 7.5% (v/v) plasma (Fig. 6a and b). The response of the BRET^6-PLR sensor to human plasmin is concentration dependent with an EC_{50} of 1.12 nM in CB (Table 1) and a limit of detection of 0.14 nM. Table 1 gives on overview of sensitivity levels. A similar detection limit of 0.18 nM, with an EC_{50} of 4.35 nM, was observed with the BRET^2-PLR sensor. Analysis of plasmin activity with the BRET^6-PLR sensor in diluted plasma (1.5% (v/v) and 7.5% (v/v)) resulted in an increase in the detection limit from 0.14 nM in CB to 0.87 and 11.90 nM, respectively. These detection limits are a 12-fold improvement for analysis carried out in 1.5% (v/v) plasma and a 5-fold improvement for analysis carried out in 7.5% (v/v) plasma when compared to analysis performed with the BRET^2-PLR sensor. It is unlikely that conformational changes of BRET^6 favour access of plasmin to its recognition site compared to the BRET^2 sensor backbone as both BRET backbones exhibit similar detection limits in buffer. Increasing the incubation time with plasmin from 10 min to 30 min led to a 43% decrease in the LOD from 0.14 nM to 0.08 nM plasmin and a 57% decrease in the EC_{50} from 1.12 nM to 0.48 nM (Table 1) for BRET^6-PLR. This improvement in detection limit is consistent with the 50% improvement in sensitivity in response to 1 nM plasmin when increasing the incubation time from 10 min to 30 min (Fig. 5b).

The red-shifted emission profile of BRET^6-PLR compared to BRET^2-PLR is less attenuated in plasma and thus produces brighter and more consistent background signals which generally offers improvements to the detection limit for measuring plasmin activity. Additionally, RLuc8, the mutagenesis template for RLuc8.6 exhibited improved stability in murine serum at 37 °C compared to native RLuc [32,33]. RLuc8.6 retains the stability of RLuc8 in cell culture and in mice [33]. It could be feasible that the optimisation round that led to RLuc8.6 also increased its stability under human plasma conditions.

3.7. Validation with biologically relevant plasmin concentrations

The linear range for detecting plasmin in plasma with BRET^6-PLR and a 10 min assay extends over 2 log units ranging from 1.24 to 11.08 nM in 1.5% plasma and 22.58–215.41 nM in 7.5% plasma. This linear range enables measurement of the relevant biological range of plasmin activity for Reteplase treatments of 0.1 U/ml to 0.6 U/ml [22] (324 nM–1946 nM plasmin for the batch used in this study). This biological range corresponds to plasmin levels of 24.3 nM–146 nM in 7.5% (v/v) plasma samples which lie within the linear range for the BRET^6-PLR calibration curve (Table 1).

Plasma samples were spiked with either 324 nM or 1946 nM and plasmin recovery rates were determined using the BRET^6-PLR sensor in 7.5% plasma (v/v) (Fig. 6). Recovery rates were 71.4 ± 8.7% (17.34 ± 2.10 nM), and 52.6 ± 4.2% (76.88 ± 6.17 nM), respectively. However, if plasmin was added after mixing diluted plasma with sensor immediately before incubation at 30 °C, recovery rates were increased to 92.7 ± 18.7% (22.52 ± 4.54 nM) and 84.9 ± 27.4% (123.96 ± 39.94 nM), for plasma samples spiked with 324 nM or 1946 nM plasmin, respectively. It is possible that natural inhibitors present in plasma such as α2-AP are interacting with the spiked plasmin in a time-dependent manner. In order to investigate this effect, recovery rates were then determined in plasma which has been incubated with plasmin on ice for 20 min. After pre-incubation on ice, recovery rates were reduced to 37.7 ± 6.5%

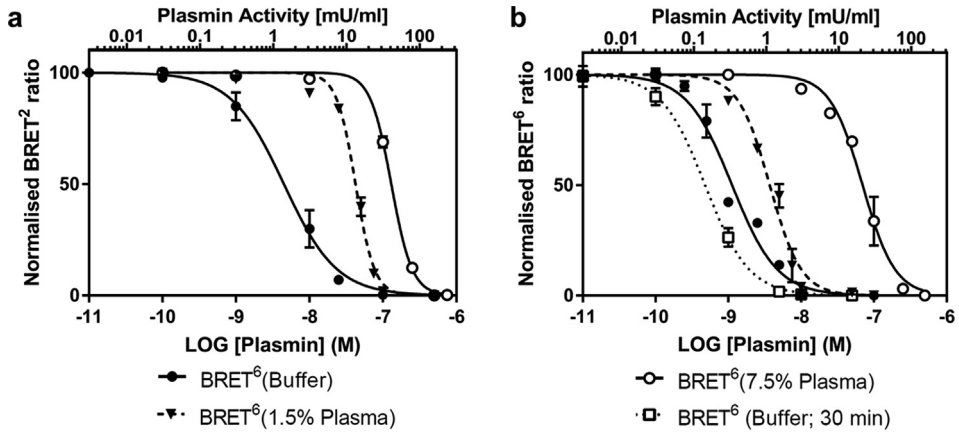

Fig. 6. Comparison of Log_{10} concentration response curves for $BRET^2$ and $BRET^6$ based plasmin sensors in buffer and human plasma.
Log_{10} concentration response curves for $BRET^2$-PLR (**a**) and $BRET^6$-PLR (**b**) plasmin sensors in plasmin cleavage buffer, 1.5% human plasma ((v/v) in buffer) and 7.5% human plasma ((v/v) in buffer) following incubation with varying concentrations of plasmin for 10 min or 30 min (only for $BRET^6$-PLR in buffer) at 30 °C. Normalised $BRET^6$ ratio's are mean ± SD (n = 3).

(8.92 ± 1.57 nM) and 25.8 ± 1.5% (37.69 ± 2.21 nM) for plasma samples spiked with 324 nM or 1946 nM plasmin, respectively. Thus, plasmin recovery rates in plasma samples are highly dependent on the incubation time of plasma with plasmin. A likely cause for this effect could be the aforementioned α2-AP. Naturally occurring α2-AP is found at concentrations of 70 μg/ml (~1 μM) in human plasma [34]. The interaction of plasmin with α2-AP can lead to an underestimation of the plasmin activity levels.

3.8. Inhibition of plasmin activity in plasma

Based on EC_{50} values, the sensitivity of plasmin sensing of $BRET^6$-PLR in CB (EC_{50}: 1.12 nM) compared to 7.5% (v/v) plasma (EC_{50}: 69.74 nM) decreases 62-fold. To further investigate the inhibition of plasmin activity by plasma, the effect of increasing concentrations of plasma on the activity of 10 nM plasmin relative to the activity in buffer was investigated (Fig. 7a).

BRET ratios were reduced by 81.8 ± 0.19% in CB while increasing amounts of plasma correlated with smaller BRET ratio responses. Plasma levels above 0.75% (v/v) (67.6 ± 1.0% BRET ratio reduction) led to a significantly lower BRET ratio reduction and only a very small response of 2.3 ± 0.8% was seen in 50% (v/v) human plasma.

To determine if α2-AP is responsible for the observed inhibition of plasmin activity by plasma, calibration curves were performed in plasma deficient of α2-AP (Fig. 7b) (Table 1). Performing calibration curves in α2-AP-deficient plasma resulted in an EC_{50} of 7.11 nM and a LOD of 1.12 nM plasmin. The EC_{50} is thus ~6.3-fold lower compared to that determined in CB (EC_{50}: 1.12 nM) but ~10-fold higher compared to that determined in human plasma containing α2-AP (EC_{50}: 67.74 nM). This infers that α2-AP is partly responsible for the inhibitory effect of plasma on plasmin activity. The 6.3 - fold decrease in EC_{50} determined in α2-AP-deficient plasma compared to that determined in buffer could be attributed to signal attenuation, other minor plasmin protease inhibitors such as α2-Macroglobulin or the higher density of proteins (Fibrinogen, Albumin) and other molecules.

3.9. Comparison with nitroanilide assay

The performance of the $BRET^6$-PLR sensor was compared to a commercially available chromogenic substrate D-Val-Leu-Lys-p-nitroanilide (D-VLK-pNA) consisting of nitroanilide (pNA) conjugated to a three amino substrate sequence specifically cleaved by plasmin. Plasmin cleaves the lysine-nitroanilide bond, releasing p-

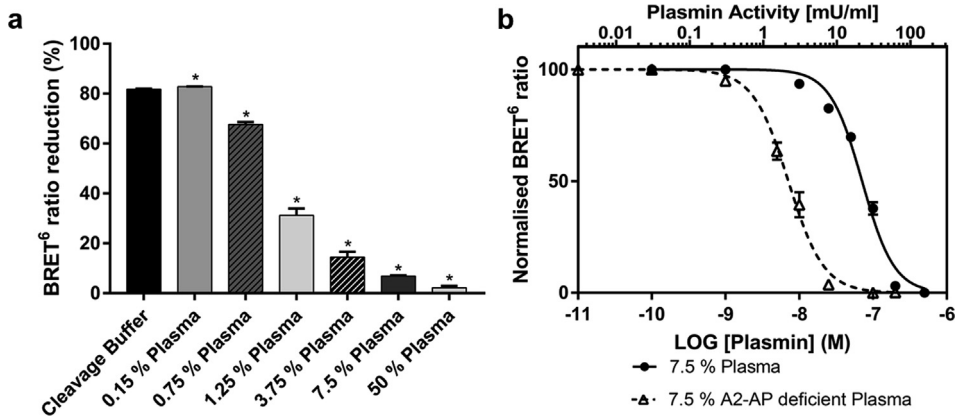

Fig. 7. Plasma inactivation of plasmin activity.
a, Analysis of $BRET^6$ ratio (mean ± SD, n = 3) of the $BRET^6$-PLR sensor following incubation with 10 nM plasmin for 10 min incubation assay at 30 °C in plasmin cleavage buffer and diluted human plasma. Statistical significance is indicated by an asterisk ($p < 0.05$) or no significance (n.s.) ($p > 0.05$). **b**, Log_{10} concentration response curves for the $BRET^6$-PLR sensor in 7.5% human plasma (v/v in buffer) and in 7.5% human plasma (v/v in buffer) deficient of α2-Antiplasmin (A2-AP). Normalised $BRET^6$ ratio's are mean ± SD (n = 3).

nitroaniline which absorbs light at 405 nm [35].

The D-VLK-pNA substrate was incubated in CB and plasma at 30 °C and the absorbance at 405 nm monitored as a function of time. For assays performed in cleavage buffer an increase in absorbance was only observed in response to the addition of plasmin while in 7.5% (v/v) plasma a continuous, increase in absorbance was observed in the absence of exogeneous plasmin. The colorigenic response in 7.5% (v/v) was not affected by the addition of 100 nM α2-AP. (Fig. S5a). This suggests that the increase in absorbance in plasma, without the addition of plasmin, is not due to the presence of naturally occurring plasmin in the plasma sample. Among its sensitivity for plasmin, the D-VLK-pNA substrate also exhibits a high sensitivity towards the protease trypsin [36] which could explain the plasmin-independent increase in absorbance as trypsin is present in human serum at a concentration of 248 ± 94.9 μg/l [37].

Calibration curves generated using the colorigenic substrate were performed in CB and in 7.5% (v/v) plasma with a 2 h incubation (Figs. S5b and c). LODs for plasmin were determined to be 2.74 nM and 10.91 nM in CB and 7.5% (v/v) plasma, respectively. The LOD in CB is thus 19.6-fold higher than that seen for BRET^6-PLR while the LOD determined in 7.5% (v/v) plasma is similar while using a 12-times shorter assay time. The BRET^6-PLR sensor offers superior performance in terms of sensitivity, selectivity and response time compared to the chromogenic substrate investigated here. This could be explained by superior signal detection of the BRET^6 system and due to a more sensitive and selective plasmin recognition site compared to D-VLK-pNA.

Jian et al. (2013) applied a fibrinolysis-based sensor to measure plasmin activity using fibrinogen-modified gold nanoparticles (Fib-Au-NPs) [38]. Plasmin-mediated cleavage of fibrinogen then leads to the aggregation of Au-NPs, due to decreased nanoparticle hydrophobicity, which can be optically measured by a colour loss. This sensor strategy achieved an LOD of 0.4 nM in a 1 h assay in highly diluted (200-fold) serum. Our sensor appears to be less affected by human blood as dilutions of 66.6-fold achieved a similar LOD (1.12 nM) while only using a 10 min incubation time. Another commercially available plasmin activity test, SensoLyte®, utilises a fluorogenic peptide. Plasmin cleavage of the peptide releases fluorescence with an excitation peak at 496 nm and emission peak at 520 nm [39]. The sensor achieves an LOD of 15 pM with an assay time of 20 min under buffer conditions. However, its sensitivity in human blood was not stated and it can be assumed that the sensitivity decreases when applied in human plasma as it requires illumination at 496 nm which triggers autofluorescent molecules in plasma such as haemoglobin and other blood components.

To the best of our knowledge, our proposed sensor exhibits the quickest assay time among all plasmin sensors while maintaining sensitive plasmin detection (Table S2).

4. Conclusion

This study is the first to compare blue and red-shifted BRET-based protease sensors in human plasma and the first report to use the BRET^6 system as a protease sensor. A novel plasmin protease recognition site combined with the beneficial signal detection of BRET^6 employed in human plasma enabled the sensor to cover the biologically relevant range of plasmin activities.

The substitution of a blue-emitting BRET system (BRET^2) with a red-shifted BRET system (BRET^6) in a plasmin sensor improved the sensitivity for measuring plasmin activity in human plasma. However, a substantial amount of the emitted light from the BRET^6 system was still absorbed by components present in plasma warranting future investigations into infra-red shifted BRET combinations to further increase sensitivities for applications in human blood [14].

A rapid test such as the 10 min assay described in this study enables the degree of fibrinolysis to be determined in near real-time and could be employed in a clinical setting during surgery for at-risk patients to better treat patients experiencing bleeding events during surgery or thrombolytic treatments. The sensor can also be used to test the levels of other fibrinolytic components affecting plasmin generation and activity such as α2-AP, plasminogen activators (tPA, uPA) or activities which are relevant biomarkers in cardiovascular diseases [40] and in cancer [41,42].

As proteases are involved in a range of diseases and physiological changes leading to their secretion or leakage into circulating blood [43], the sensing approach described here also has the potential for application to diagnosing and monitoring other pathologies by tuning the sensitivity and selectivity of the protease recognition site between RLuc8.6 and TurboFP635 for detection of a range of physiologically relevant protease biomarkers.

Credit author statement

Felix Weihs: Conceptualization, Methodology, Investigation, Validation, Formal analysis, Visualization, Writing - review & editing. Alex Peh: Investigation. Helen Dacres: Conceptualization, Methodology, Formal analysis, Writing - review & editing

Declaration of competing interest

The authors declare that they have no known competing financial interests or personal relationships that could have appeared to influence the work reported in this paper.

Appendix A. Supplementary data

Supplementary data to this article can be found online at https://doi.org/10.1016/j.aca.2019.12.044.

References

[1] M.J. Daley, M.S. Murthy, E.J. Peterson, Bleeding risk with systemic thrombolytic therapy for pulmonary embolism: scope of the problem, Ther. Adv. Drug Saf. 6 (2) (2015) 57–66.
[2] P.J. Declerck, H. Moreau, J. Jespersen, J. Gram, C. Kluft, Multicenter evaluation of commercially available methods for the immunological determination of plasminogen activator inhibitor-1 (PAI-1), Thromb. Haemost. 70 (5) (1993) 858–863.
[3] A.R. Folsom, M. Cushman, S.R. Heckbert, W.D. Rosamond, N. Aleksic, Prospective study of fibrinolytic markers and venous thromboembolism, J. Clin. Epidemiol. 56 (6) (2003) 598–603.
[4] N.H. van Tilburg, F.R. Rosendaal, R.M. Bertina, Thrombin activatable fibrinolysis inhibitor and the risk for deep vein thrombosis, Blood 95 (9) (2000) 2855–2859.
[5] N. Alkjaersig, A.P. Fletcher, S. Sherry, The mechanism of clot dissolution by plasmin, J. Clin. Investig. 38 (7) (1959) 1086–1095.
[6] H.S. Rollema, S. Visser, J.K. Poll, Spectrophotometric assay of plasmin and plasminogen in bovine-milk, Milchwissenschaft 38 (4) (1983) 214–217.
[7] B.C. Richardson, K.N. Pearce, The determination of plasmin in dairy-products, New Zeal J. Dairy Sci. 16 (3) (1981) 209–220.
[8] X. Xu, M. Soutto, Q. Xie, S. Servick, C. Subramanian, A.G. von Arnim, C.H. Johnson, Imaging protein interactions with bioluminescence resonance energy transfer (BRET) in plant and mammalian cells and tissues, Proc. Natl. Acad. Sci. U. S. A. 104 (24) (2007) 10264–10269.
[9] Z. Xia, Y. Xing, M.K. So, A.L. Koh, R. Sinclair, J. Rao, Multiplex detection of protease activity with quantum dot nanosensors prepared by intein-mediated specific bioconjugation, Anal. Chem. 80 (22) (2008) 8649–8655.
[10] H. Dacres, M.M. Dumancic, I. Horne, S.C. Trowell, Direct comparison of bioluminescence-based resonance energy transfer methods for monitoring of proteolytic cleavage, Anal. Biochem. 385 (2) (2009) 194–202.
[11] H. Dacres, M.M. Dumancic, I. Horne, S.C. Trowell, Direct comparison of fluorescence- and bioluminescence-based resonance energy transfer methods for real-time monitoring of thrombin-catalysed proteolytic cleavage, Biosens. Bioelectron. 24 (5) (2009) 1164–1170.
[12] H. Dacres, J. Wang, A. Anderson, T.S.C., A rapid and sensitive biosensor for measuring plasmin activity in milk, Sens. Actuators B Chem. 301 (2019).

[13] F. Morgner, S. Stufler, D. Geissler, I.L. Medintz, W.R. Algar, K. Susumu, M.H. Stewart, J.B. Blanco-Canosa, P.E. Dawson, N. Hildebrandt, Terbium to quantum dot FRET bioconjugates for clinical diagnostics: influence of human plasma on optical and assembly properties, Sens. Basel 11 (10) (2011) 9667–9684.
[14] F. Weihs, H. Dacres, Red-shifted bioluminescence Resonance Energy Transfer: improved tools and materials for analytical in vivo approaches, Trac. Trends Anal. Chem. 116 (2019) 61–73.
[15] F. Li, J. Yu, Z. Zhang, Z. Cui, D. Wang, H. Wei, X.E. Zhang, Use of hGluc/tdTomato pair for sensitive BRET sensing of protease with high solution media tolerance, Talanta 109 (2013) 141–146.
[16] R. Arts, I. den Hartog, S.E. Zijlema, V. Thijssen, S.H. van der Beelen, M. Merkx, Detection of antibodies in blood plasma using bioluminescent sensor proteins and a smartphone, Anal. Chem. 88 (8) (2016) 4525–4532.
[17] Y. Ni, R. Arts, M. Merkx, Ratiometric bioluminescent sensor proteins based on intramolecular split luciferase complementation, ACS Sens. 4 (1) (2018) 20–25.
[18] B.R. Branchini, D.M. Ablamsky, J.C. Rosenberg, Chemically modified firefly luciferase is an efficient source of near-infrared light, Bioconjug. Chem. 21 (11) (2010) 2023–2030.
[19] A. Dragulescu-Andrasi, C.T. Chan, A. De, T.F. Massoud, S.S. Gambhir, Bioluminescence resonance energy transfer (BRET) imaging of protein-protein interactions within deep tissues of living subjects, Proc. Natl. Acad. Sci. U. S. A. 108 (29) (2011) 12060–12065.
[20] V.M. Rauh, M. Bakman, R. Ipsen, M. Paulsson, A.L. Kelly, L.B. Larsen, M. Hammershoj, The determination of plasmin and plasminogen-derived activity in turbid samples from various dairy products using an optimised spectrophotometric method, Int. Dairy J. 38 (1) (2014) 74–80.
[21] G.L. Long, J.D. Winefordner, Limit of detection, Anal. Chem. 55 (7) (1983). A712-+.
[22] T.W. Stief, A. Richter, R. Bunder, B. Maisch, H. Renz, Monitoring of plasmin and plasminogen activator activity in blood of patients under fibrinolytic treatment by reteplase, Clin. Appl. Thromb. Hemost. 12 (2) (2006) 213–218.
[23] Mj Weinstei, Doolittl Rf, Differential specificities of thrombin, plasmin and trypsin with regard to synthetic and natural substrates and inhibitors, Biochim. Biophys. Acta 258 (2) (1972), 577-&.
[24] P.L.H. Mcsweeney, N.F. Olson, P.F. Fox, A. Healy, P. Hojrup, Proteolytic specificity of plasmin on bovine alpha-S1-casein, Food Biotechnol. 7 (2) (1993) 143–158.
[25] L.S. Hervio, G.S. Coombs, R.C. Bergstrom, K. Trivedi, D.R. Corey, E.L. Madison, Negative selectivity and the evolution of protease cascades: the specificity of plasmin for peptide and protein substrates, Chem. Biol. 7 (6) (2000) 443–453.
[26] T. Forster, *Zwischenmolekulare energiewanderung und fluoreszenz, Ann. Phys. Berlin 2 (1–2) (1948) 55–75.
[27] M. Chalfie, Y. Tu, G. Euskirchen, W.W. Ward, D.C. Prasher, Green fluorescent protein as a marker for gene expression, Science 263 (5148) (1994) 802–805.
[28] T. Iizasa, T. Fujisawa, M. Suzuki, S. Motohashi, K. Yasufuku, T. Yasukawa, M. Baba, M. Shiba, Elevated levels of circulating plasma matrix metalloproteinase 9 in non-small cell lung cancer patients, Clin. Cancer Res. 5 (1) (1999) 149–153.
[29] P.N. Walsh, S.S. Ahmad, Proteases in blood clotting, Essays Biochem. 38 (2002) 95–111.
[30] T.W. Stief, Specific determination of plasmatic thrombin activity, Clin. Appl. Thromb. Hemost. 12 (3) (2006) 324–329.
[31] K.N. Lee, K.W. Jackson, V.J. Christiansen, K.H. Chung, P.A. McKee, Alpha2-antiplasmin: potential therapeutic roles in fibrin survival and removal, Curr. Med. Chem. Cardiovasc. Hematol. Agents 2 (4) (2004) 303–310.
[32] A.M. Loening, T.D. Fenn, A.M. Wu, S.S. Gambhir, Consensus guided mutagenesis of Renilla luciferase yields enhanced stability and light output, Protein Eng. Des. Sel. 19 (9) (2006) 391–400.
[33] A.M. Loening, A.M. Wu, S.S. Gambhir, Red-shifted Renilla reniformis luciferase variants for imaging in living subjects, Nat. Methods 4 (8) (2007) 641–643.
[34] M. Moroi, N. Aoki, Isolation and characterization of alpha2-plasmin inhibitor from human plasma. A novel proteinase inhibitor which inhibits activator-induced clot lysis, J. Biol. Chem. 251 (19) (1976) 5956–5965.
[35] P. Friberger, M. Knos, S. Gustavsson, L. Aurell, G. Claeson, Methods for determination of plasmin, antiplasmin and plasminogen by means of substrate S-2251, Haemostasis 7 (2–3) (1978) 138–145.
[36] N.U. Bang, L.E. Mattler, Sensitivity and specificity of plasma serine protease chromogenic substrates, Haemostasis 7 (2–3) (1978) 98–104.
[37] J.M. Artigas, M.E. Garcia, M.R. Faure, A.M. Gimeno, Serum trypsin levels in acute pancreatic and non-pancreatic abdominal conditions, Postgrad. Med. J. 57 (666) (1981) 219–222.
[38] J.W. Jian, W.C. Chiu, H.T. Chang, P.H. Hsu, C.C. Huang, Fibrinolysis and thrombosis of fibrinogen-modified gold nanoparticles for detection of fibrinolytic-related proteins, Anal. Chim. Acta 774 (2013) 67–72.
[39] SensoLyte ® Rh110 Plasmin Activity Assay Kit *Fluorimetric* (accessed May 2019), https://www.anaspec.com/products/product.asp?id=48255.
[40] H. Matsuno, Alpha2-antiplasmin on cardiovascular diseases, Curr. Pharmaceut. Des. 12 (7) (2006) 841–847.
[41] C. Duggan, S. Kennedy, M.D. Kramer, C. Barnes, P. Elvin, E. McDermott, N. O'Higgins, M.J. Duffy, Plasminogen activator inhibitor type 2 in breast cancer, Br. J. Canc. 76 (5) (1997) 622–627.
[42] J.H. de Witte, C.G. Sweep, J.G. Klijn, N. Grebenschikov, H.A. Peters, M.P. Look, T.H. van Tienoven, J.J. Heuvel, J. Bolt-De Vries, T.J. Benraad, J.A. Foekens, Prognostic value of tissue-type plasminogen activator (tPA) and its complex with the type-1 inhibitor (PAI-1) in breast cancer, Br. J. Canc. 80 (1–2) (1999) 286–294.
[43] C. Lopez-Otin, J.S. Bond, Proteases: multifunctional enzymes in life and disease, J. Biol. Chem. 283 (45) (2008) 30433–30437.